

Description of a dimethylmercury automatic analyzer for the high-resolution measurement of dissolved gaseous mercury species in surface ocean waters

Yipeng He ^a, Xiangming Shi ^a, Wesley W. Huffman ^a, Carl H. Lamborg ^b, Robert P. Mason ^{a*}

^a Department of Marine Sciences, University of Connecticut, 1080 Shennecossett Road, Groton, Connecticut 06340, USA

^b Ocean Sciences Department, University of California Santa Cruz, 1156 High Street, Santa Cruz, California 95064, USA

**Email: robert.mason@uconn.edu*

Website: <https://mason.mercury.uconn.edu>

Submit to: Environmental Sciences & Technology

*To Whom Correspondence Should be Addressed

1 **Abstract**

2 Our understanding of the significance of dimethylmercury (DMHg) to the mercury (Hg) the
3 global ocean biogeochemical cycle is unclear because of the lack of detailed DMHg
4 measurements in the water column. To our knowledge, 30-years of published studies have
5 generated no more than 200 DMHg data points in the ocean surface waters and marine boundary
6 layer (MBL). To improve the precision and reduce the uncertainty in determining DMHg in
7 surface seawater, we developed a simple and robust DMHg automatic analyzer (DAA). This
8 DAA system couples the main sampling and analytic steps, including a continuous flow
9 chamber, with dual Carbotrap pre-concentration, a gas chromatographic column, a cold vapor
10 atomic fluorescence spectrometry and a data logger for signal integration. We compared the
11 operation, performance, and reproducibility between our DAA and the traditional manual
12 analytic method. Its advantages include the ease of operation, the high time resolution and
13 precision (30 min sampling; < 5% relative variation) and long-term stability (two weeks). The
14 DAA can determine DMHg in both the MBL and surface seawater. The estimated detection
15 limits for DMHg with the DAA in atmosphere and in surface seawater are 10 pg/m³ and 0.2 fM,
16 respectively. The successful DAA field measurement in coastal waters indicates that it can help
17 detect the low DMHg concentration in surface seawater and the time series DMHg data helped
18 our understanding of the DMHg behavior (sources and sinks) and its flux into the MBL. The
19 comparison of DMHg concentration in various oceans also suggests that the coastal region had
20 the lowest averaged DMHg; up to an order of magnitude lower than other ecosystems.

21

22 **Keywords**

23 Dimethylmercury, Dissolved gaseous mercury, Automatic analyzer, High time resolution,
24 Marine boundary layer, Coastal waters

25

26 **Synopsis**

27 This study describes a newly developed dimethylmercury (DMHg) automatic analyzer and
28 presents the first high-resolution DMHg observations in the surface ocean, demonstrating its
29 usefulness for examining DMHg behavior and its role in the global biogeochemical cycling of
30 mercury.

31

32 **Introduction**

33 Dimethylmercury (DMHg), a volatile, toxic and organic form of mercury (Hg), appears
34 to be relatively ubiquitous in marine waters and has been found in deep hypoxic oceanic waters,
35 upwelling waters, coastal waters and the mixed layer, primarily under upwelling conditions, in
36 all oceans globally.¹⁻¹¹ From the Hg cycling perspective, DMHg could be formed by Hg
37 methylation in water column and/or in benthic sediment through biotic and abiotic processes
38 which are, however, still unclear in terms of their importance.¹²⁻¹⁴ Although current
39 understanding of the sources of DMHg in oceanic waters is limited, the degradation of DMHg
40 may be an important source of monomethylmercury (MMHg) in the marine environment and the
41 marine boundary layer (MBL) atmosphere, and in wet deposition.^{9, 15, 16} From a human health
42 perspective, MMHg is the most bioaccumulative form of Hg in marine food webs and the form
43 which impacts human Hg exposure through seafood consumption.^{17, 18} Previous studies suggest
44 that DMHg ranges from 30% to 80% of the total methylated Hg pool (both MMHg and DMHg)
45 in ocean waters, which means degradation of DMHg to MMHg could also indirectly contribute
46 to the marine food web MMHg accumulation.^{6, 15} In addition, it has been suggested that DMHg
47 could evade from the surface ocean as a gas or within sea spray into the MBL atmosphere.¹⁹⁻²¹
48 The evaded DMHg, after decomposition to MMHg, can be absorbed by water vapor contributing
49 to the methylated Hg compounds in the rain in coastal regions, in the snow in polar regions, or in
50 open ocean locations, and could be an important MMHg source.²¹⁻²³ However, due to the limited
51 data on DMHg levels in surface waters and the MBL, it's difficult to understand the behavior
52 and importance of DMHg's role within the global Hg biogeochemical cycle.

53 Based on our knowledge, the past 30-years of published studies have generated no more
54 than 200 data points of DMHg within the surface ocean/MBL and no more than 1000 data points
55 of DMHg from the entire water column in all oceans.^{1-11, 24} The reasons for the limited dataset of
56 DMHg are that: 1) DMHg is not stable after collection in bottles and degrades within hours and
57 so needs to be analyzed on board or immediately after collection; and 2) DMHg concentrations
58 are generally low and near current detection limits in surface water and much of the interior
59 ocean, except for some atypical regions (i.e., Arctic, Antarctic, low oxygen zones and upwelling
60 waters).^{15, 25} Given its low concentration, and the traditional manual analytic method for its
61 measurement includes several steps, such as collection of a large volume of seawater and pre-
62 concentration of DMHg to improve the detection limit (DL) prior to the analysis. However, this

63 may also increase the uncertainty and operational bias. Furthermore, the long purging time
64 during the preconcentration step may also promote DMHg degradation in the purging bottle.
65 Thus, in many ocean studies of Hg speciation, analysis of DMHg is not done and samples are
66 acidified for later analysis of methylated Hg. Acidification converts the DMHg into the more
67 stable MMHg and allows for the determination of total methylated Hg.

68 To briefly summarize, the traditional manual analytic method for determination of DMHg
69 is based on sparging a water sample with pre-concentration on a solid phase absorbent, either a
70 Tenax[®] or Carbotrap[®] trap, followed by thermal desorption, gas chromatographic (GC)
71 separation, decomposition of Hg species to elemental Hg (Hg⁰) and detection.²⁶ Several detection
72 methods for quantifying Hg⁰ have been successfully tested and used with this manual method,
73 such as cold vapor atomic absorption spectrometry (CVAAS),^{27, 28} cold vapor atomic
74 fluorescence spectrometry (CVAFS),²⁶ and inductively coupled plasma mass spectrometry
75 (ICPMS).^{29, 30} However, despite the detection methods used, this traditional manual analytical
76 method requires intensive effort, and is not suitable for continuous or semi-continuous
77 measurement. In addition, there is potential bias of the results from this manual method,
78 primarily due to: 1) purging gas leaks; 2) trap contamination; and 3) operational failure, (i.e., trap
79 overheating and degradation, baseline drift, biased calibration spikes). Additionally, the DL in
80 previous studies varies widely from 2 fM to 25 fM, although these previous studies all use the
81 traditional manual method.^{5, 24, 25, 31} Therefore, a new method is urgently needed for improving
82 the precision and the DL in determining DMHg in the ocean, to confirm or refute its importance
83 in the global Hg cycle by determining its concentration at a high resolution in both time and
84 space.

85 In this study, we describe a simple and robust DMHg automatic analyzer (DAA), which
86 is newly developed and tested in laboratory and field. This DAA is based on the automation of
87 the existing manual method. This method minimizes the uncertainty of conventional procedures,
88 minimizes the labor requirements of the manual analysis and improves the accuracy and DL of
89 DMHg determination. More specifically, the advantages of our DAA include: 1) the ease of
90 operation (program controlled); 2) its high time resolution (30 min collection per data point); and
91 3) its high precision (< 5% relative variation), low DL (0.2 fM in water) and long-term
92 operational stability (two weeks). The DAA is applicable to the determination of DMHg in both
93 the atmosphere and the surface seawater to allow for examination of air-sea exchange at the

94 MBL/seawater interface. The estimated detection limits for DMHg using the DAA in the
95 atmosphere and in surface seawater are 10 pg/m^3 and 0.2 fM , respectively. The successful field
96 measurement with our DAA indicates that the high-resolution measurements and low DL can
97 help us detect the temporal variability in low DMHg concentration in surface seawater. With a
98 time-series of DMHg data, we also demonstrate how such data can lead to a better understanding
99 of DMHg behavior and its flux from surface seawater to the atmosphere.

100

101 **Materials and Methods**

102 **Caution:** Dimethylmercury is a volatile and extremely toxic organic Hg compound. It has been
103 shown to cause human death through contact with the skin from one droplet of a concentrated
104 dimethylmercury solution.^{32,33} Additionally, nitrile and other material gloves can be penetrated
105 by dimethylmercury liquid as it should be considered as an organic compound. Therefore, we do
106 not recommend working with concentrated or pure solutions. All work needs to be performed
107 under the protection of an evacuated fume hood with extreme caution and suitable protective
108 equipment. However, given the extremely low concentrations of dimethylmercury in the
109 environment (fM), there is no danger from making these environmental measurements.

110

111 **Experimental apparatus.** The design of the DAA is shown in Figure 1a, in contrast to
112 the traditional manual analytic method, which is depicted in Figure 1b. For measuring dissolved
113 gaseous Hg species (DGHg) in seawater, which includes both Hg^0 and DMHg, a continuous
114 counter-flow chamber has been coupled with the DAA. This approach has been used in many
115 studies of DGHg.³⁴⁻³⁶ The principle of the continuous flow chamber is that the opposite flow of
116 gas in the chamber can facilitate the exchange and rapid equilibration of dissolved gaseous Hg
117 species between the aqueous and gaseous phase.³⁴ A similar approach is used in most studies of
118 dissolved gases in environmental waters. To briefly summarize, the continuous flow chamber
119 contains a seawater filled jacketed outer cylinder made of acrylic, which helps maintain the
120 temperature of the inner cylinder filled with seawater to that of the environmental sampled water.
121 The water flow is into the inner chamber followed by the outer chamber. Pressurized air (Hg
122 free) is directed by Teflon tubing to glass frits ($70\text{-}100 \text{ }\mu\text{m}$ porosity, Ace Glass, MilliporeSigma
123 Corp.) mounted into the bottom of the inner cylinder at a flow rate of 1.1 to 1.2 L/min. The glass
124 frits disperse the pressurized air into fine bubbles which contacts the seawater increasing the

125 contact area between the air and seawater and increasing the efficiency of equilibration of the
126 gases in the seawater with the sparging air. The seawater flows into the inner cylinder from
127 above and exits at the bottom of the inner cylinder at a flow rate of 10 to 15 L/min. The ratio of
128 water to air flow determines the response time of the system to changes in water concentration.³²
129 The height of seawater at the outflow port of the outer cylinder determines the seawater level at
130 the inner cylinder and keeps it relatively stable. In addition, a temperature sensor (HOBO
131 MX2201, Onset Computer Corp.) was installed in the inner cylinder to record the seawater
132 temperature. After gaseous Hg species reach equilibrium between the aqueous and gaseous
133 phase, the gaseous Hg species are then collected onto the sampling trap from the outgoing air.
134 This continuous flow chamber has been successfully used for determining dissolved Hg⁰ in
135 surface seawater and its flux in previous studies in the Pacific, Atlantic, Arctic and coastal
136 oceans.³⁵⁻³⁷

137 The outgoing air from the continuous flow chamber is dried using soda lime (4-8 mesh,
138 Alfa Aesar) and directed into the DAA and a Tekran 2537B for determining DMHg and Hg⁰,
139 respectively (Figure 1a). As with the traditional manual method, the outgoing air from the
140 continuous flow chamber passes through a Carbotrap with removes organic Hg compounds
141 primarily (Figure 1b). The manual method requires changing the Carbotrap every 2 hr at the
142 typical 1 L/min flow rate to minimize the breakthrough of DMHg from the Carbotrap.³⁸ For the
143 DAA, dual Carbotrap tubes (Carbotrap B, 20-40 mesh, Supelco) are designed to allow the
144 alternation between the adsorption and desorption of DMHg with each sampling cycle. For
145 example, while Carbotrap A is sampling, the outgoing air from the continuous flow chamber
146 passes through the Carbotrap A for adsorption of DMHg and then passes into Tekran 2537B for
147 determining of Hg⁰. At the end of the sampling cycle for Carbotrap A, the sampling air flow
148 switches to Carbotrap B and initializes the sampling cycle for Carbotrap B. Then Carbotrap A
149 enters the desorption cycle with a continuous argon (UHP, Airgas Inc.) purging flow at 60
150 ml/min controlled by the mass flow controller (MFC). The Carbotrap A is also heated to 250 °C
151 for 30 sec using the nichrome resistance wire coil, wrapped around the trap. The argon carries
152 any desorbed Hg species from Carbotrap A to the isothermal gas chromatographic column (GC;
153 Teflon tube, 1 m length, ¼ inch OD; packed with Chromosorb WAW-DMCS 60-80 mesh, 15%
154 OV-3, Supelco), maintained at the temperature of 38 ± 1 °C. The Hg species are separated by the
155 GC column based on their molecular weight, and all forms are decomposed to Hg⁰ in the

156 pyrolyzer column after the GC column. The pyrolyzer column is a quartz tube (15 cm length, ¼
157 inch OD; packed with quartz wool) which is heated and kept at 700 ± 50 °C by a nichrome
158 resistance wire coil inside a thermally insulated oven. After the Hg species are converted to Hg^0
159 by the pyrolyzer, the produced Hg^0 passes through the CVAFS commercial detector – a Tekran
160 2500 is used in this application. The voltage information from the CVAFS and the peak area is
161 recorded and integrated by a PeakSimple Chromatography Data System (Model 333, SRI
162 Instruments Inc.). The algorithm of the peak integration includes two steps: 1) location of the
163 peak start and end points by fitting the whole voltage information spectrum using a log normal
164 distribution equation; and 2) integrating the peak area between the peak start and end points.
165 Additional algorithm details of peak integration system are included in the Supporting
166 Information (S1; Figure S1). The entire cycle from thermal desorption of the Carbotrap to peak
167 data acquisition is about 5 min. The entire sampling cycle is designed to be 30 min, which
168 represents a total of 30 L of air passing through the Carbotrap at 1 L/min flow rate. The sampling
169 cycle and desorption cycle is controlled by a programable script which mainly commands the
170 solenoid valve (NResearch Inc.), the nichrome resistance wire and the cooling fan during
171 switching between each Carbotrap. For calibrating the DAA, with either Hg^0 or DMHg, there is
172 an injection port for manually injecting gaseous Hg species prior to the port V2 (shown in Figure
173 1a). All tubing and connectors are Teflon with ¼ inch OD, unless elsewhere stated. The DAA
174 setting and analytical parameters are summarized in Table 1. The use of DAA improves the
175 analytical efficiency by allowing analysis without supervision and also allows high time
176 resolution measurement.

177
178 **Laboratory validation.** The solid phase adsorbent for DMHg used in the DAA is the
179 commercial Carbotrap B, which has a high and stable recovery about $100 \pm 0.3\%$ for DMHg.³⁸
180 However, a known issue for the Carbotrap material is the potential breakthrough of DMHg,
181 which usually occurs with increasing sampling volume causing loss of the analyte from the trap.
182 Therefore, the volume of air that can pass through the adsorbent without any significant loss of
183 analyte needs to be determined. The breakthrough volume of the Carbotrap was determined by
184 the traditional manual method as shown in Figure 1b. From previous studies, it has been
185 demonstrated that the seawater in the continuous flow chamber has a relative stable DMHg
186 concentration over short timescales. While increasing the sampling air volume from 10 to 400 L,

187 adsorbed DMHg on the Carbotrap was measured by the GC-CVAFS system. Additional details
188 of the breakthrough sampling period study are included in the Supporting Information Figure S2.
189 The breakthrough recovery was calculated from this data, and compared with previous studies as
190 shown in Figure 2a, which demonstrated that the larger sampling volumes used resulted in a
191 lower recovery of DMHg. The fitted regression curve indicated that the sampling volume should
192 not be larger than 90 L to ensure a good recovery (> 95%).

193 The retention time of DMHg in the DAA was determined by injecting DMHg vapor
194 directly into the system. The DMHg vapor was obtained by sampling the headspace of a diluted
195 DMHg solution with a glass syringe (Hamilton Comp.). The diluted DMHg solution was handled
196 carefully in an evacuated fume hood. The retention time for Hg⁰ and DMHg were 75 sec and 160
197 sec, respectively. The detection limit (DL), determined as 3 times of the standard deviation of
198 multiple analysis of a known amount of DMHg, is 0.3 pg for the DAA. According to the chosen
199 sampling duration of 30 min at 1 L/min, the DL for the atmosphere is 10 pg/m³. The calibration
200 of the DAA can be implemented in two ways: 1) by injecting known amounts of DMHg vapor;
201 and 2) by changing the Carbotrap with a gold trap and injecting known amounts of Hg⁰ vapor.
202 The calibration curve was found to have a similar response in terms of the peak area and Hg
203 mass for both DMHg injection and Hg⁰ injection (< 10% relative variation). Therefore, we
204 assumed that, for the DAA system, the peak area response would be the same in the GC-CVAFS
205 for the two gaseous Hg species, because DMHg is thermally decomposed to Hg⁰ prior to the
206 detection. Due to the toxicity of DMHg, it is impossible to transport and use the DMHg standard
207 to calibrate the DAA in the field. Instead of using a DMHg standard, it is much safer to transport
208 and use a Hg⁰ standard to calibrate the DAA. The DAA was calibrated every three days to
209 evaluate the stability of the DAA, as shown in Figure 2b. The result of this multiple calibration
210 suggested that the DAA system could run stably (< 5% relative variation) without extra care and
211 supervision for more than two weeks.

212
213 **Field measurement.** Prior to the field measurement, the DAA system blank was
214 determined by pumping tap water into the continuous flow chamber. The calculated blank for the
215 dissolved DMHg was below the DL, while the calculated blank for dissolved Hg⁰ was < 7 fM.
216 The field measurement site was located within the Rankin Lab, a flowing seawater facility at the

217 University of Connecticut, Avery Point campus, which is on the east side of Long Island Sound
218 and connected to the North Atlantic, as shown in Figure 3a.

219 The seawater was pumped from the surface waters of Long Island Sound (< 5 m depth)
220 into the continuous flow chamber at a flow rate of 10-15 L/min to ensure that equilibrium is
221 rapidly obtained and that the water is not depleted of DMHg.³⁴ The outgoing air at a flow rate of
222 1.0-1.2 L/min passed through both the DAA and Tekran 2537B for quantifying both the
223 dissolved DMHg and Hg⁰, respectively. The ratio of the seawater flow and air flow was set
224 around 10, which has been tested in the lab experiments and also used in the previous cruises.³⁴
225 ³⁷ After quantifying the different amounts of Hg species on the trap, each component of
226 dissolved gaseous Hg species can be recalculated from its corresponding concentration in the
227 outgoing air using the following equations and Henry's Law:

$$228 \quad Hg_{diss}^0 = \frac{Hg_{air}^0}{H_{Hg^0}}$$
$$229 \quad DMHg_{diss} = \frac{DMHg_{air}}{H_{DMHg}}$$

230 where Hg_{air}^0 and $DMHg_{air}$ represent corresponding Hg species concentration in the outgoing air
231 and H_{Hg^0} and H_{DMHg} are the dimensionless Henry's law constant for Hg⁰ and DMHg,
232 respectively. The Henry's law constant is temperature dependent, and the detailed calculation
233 can be found in Supporting Information Table S1. The estimation of gas exchange flux could
234 also be carried out using the following equations

$$235 \quad F_{Hg^0} = k_{w,Hg^0} \left(Hg_{diss}^0 - \frac{C_{air,Hg^0}}{H_{Hg^0}} \right)$$
$$236 \quad F_{DMHg} = k_{w,DMHg} \left(DMHg_{diss} - \frac{C_{air,DMHg}}{H_{DMHg}} \right)$$

237 where C_{air,Hg^0} and $C_{air,DMHg}$ represent corresponding Hg species concentrations in the ambient
238 atmosphere and k_{w,Hg^0} and $k_{w,DMHg}$ are the mass transfer coefficient for Hg⁰ and DMHg,
239 respectively. The mass transfer coefficient is both temperature and wind speed dependent, and
240 again the detailed calculation of their values for Hg⁰ and DMHg can be found in Supporting
241 Information Table S1. As the Carbotrap can potentially absorb a small amount of Hg⁰, which is
242 quantified because of the GC separation of species, the calculation of the Hg⁰ amount required
243 consideration of both the Hg⁰ absorbed by the Carbotrap and gold trap. The raw data of

244 measured dissolved Hg⁰ and DMHg amounts has been converted to a 5-hour moving average to
245 minimize the impact of the outlier values and demonstrate the longer-term trends. The
246 atmospheric Hg⁰ concentration at the sampling site was measured by a Tekran 2537X, while the
247 atmospheric DMHg concentration at the sampling site was found to be under the DL. Therefore,
248 the DMHg flux calculation was based only on the dissolved DMHg concentration in surface
249 seawater. In addition to comparing and evaluating the collected data for both DMHg and Hg⁰,
250 the DMHg measurements in Long Island Sound were also been compared with previous studies
251 in Arctic, Pacific and Atlantic to quantitatively illustrate the DMHg distribution in surface waters
252 globally. The implications of its concentration and flux are evaluated within the context of the
253 global Hg biogeochemical cycle.

254
255 **Auxiliary data.** In order to understand the extent to which environmental factors
256 influenced the dissolved gaseous Hg species, several environmental parameters (i.e., surface
257 seawater temperature, atmospheric temperature, wind direction and wind speed) were monitored
258 by the weather station located at University of Connecticut, Avery Point campus, near the
259 Rankin Lab. Environmental parameters collected are summarized and shown in Supporting
260 Information Figure S3.

261 262 **Results and discussion**

263 **Validation of the DAA.** Several optimizations of the DAA system have already resulted
264 in improved accuracy, higher reproducibility, a low DL, and long-term continuous analysis.

265 The solid phase adsorbent for DMHg used in the DAA is the commercial Carbotrap B,
266 which has a high and stable recovery about $100 \pm 0.3\%$ for DMHg.³⁸ The breakthrough issue for
267 Carbotrap B was quantified and is shown in Figure 2a, with a comparison to previous studies.
268 The calculated overall breakthrough recovery fitted a polynomial curve ($R^2 = 0.96$, $p <$
269 0.001 ***), illustrating that increasing sampling volume would cause a lower recovery. We
270 conclude that, for a good recovery (> 95%), the sampling volume should not be larger than 90 L,
271 or 90 min for a sampling rate at 1 L/min. Here, the sampling time in our study is much shorter
272 (30 min).

273 The gaseous Hg species are identified by their retention times after the GC column
274 separation. The performance of the peak separation is dependent on: 1) the carrier gas flow rate;

275 and 2) the GC column temperature. Optimization of the DAA showed that the good separation of
276 peaks is achieved with a carrier flow of 60 ± 2 ml/min and a GC column temperature of $38 \pm$
277 1 °C. Therefore, the optimized retention time for Hg^0 and DMHg was determined as 75 sec and
278 160 sec, respectively (as shown in Supporting Information Figure S1).

279 The estimated DL for DMHg with the DAA in atmosphere and in surface seawater are 10
280 pg/m^3 and 0.2 fM, respectively. The DLs in previous studies have varied widely from 2 fM to 25
281 fM.^{5, 24, 25, 31} Thus, our DAA is a substantial improvement with a 10 times lower DL. In addition,
282 the calibration can be easily done by injecting Hg^0 vapor into the DAA system (changing
283 Carbotrap to gold trap is required). Due to the toxicity of DMHg, it will be much safer to carry
284 and use Hg^0 standard to calibrate the DAA on the field measurement. Based on our continuous
285 calibrations (every three days), the DAA is stable with the averaged variation of $100 \pm 3\%$ (as
286 shown in Figure 2b; $< 5\%$ relative variation) without supervision for more than two weeks.

287
288 **Field measurement.** The sampling site is located at the eastern end of Long Island
289 Sound, near the mouth of the Thames River (Figure 3a). The seawater exchange, and mixing
290 between fresh river water and salty seawater may drive a higher Hg methylation potential and the
291 formation of DMHg in the vicinity of the sampling location, as found by Schartup et al.³⁹ Also,
292 there is the potential for Hg methylation within the sediment and its transport to the water
293 column at the shallow sampling location through porewater diffusion or sediment resuspension.⁴⁰
294 Previous studies that have investigated dissolved methylated Hg in the Long Island Sound water
295 column have focused mostly on MMHg, not DMHg, over the past 20 years.^{41, 42} Therefore, the
296 understanding of the role of DMHg flux in the Hg biogeochemical cycling in the coastal region
297 like Long Island Sound represents a knowledge gap. Data on DMHg in the open ocean is also
298 limited.

299 Here, we present the high time resolution continuous measurements of gaseous Hg
300 species in both the surface seawater and atmosphere in Long Island Sound. Dissolved DMHg
301 and Hg^0 in surface seawater were determined with a resolution of 30 min and 5 min,
302 respectively, and averaged 2.7 ± 0.7 pmol/m^3 ($n = 333$) and 95.0 ± 16.3 pmol/m^3 ($n = 2016$),
303 respectively, as shown in Figure 3b and Figure 3c. The estimated air-sea exchange flux for
304 DMHg and Hg^0 were calculated as 0.12 ± 0.14 $\text{pmol}/\text{m}^2\text{-hr}$ ($n = 333$) and 4.79 ± 3.80 $\text{pmol}/\text{m}^2\text{-hr}$
305 ($n = 2016$) as shown in Figure 3d and Figure 3e. The magnitude of dissolved Hg^0 was about 30

306 times higher than dissolved DMHg in surface seawater at this location. Gosnell, et al.⁴³
307 measured a concentration of total methylated Hg in eastern LIS of 15 ± 9 pmol/m³, which
308 suggests that the relative amount of DMHg is small compared to MMHg at this location. This is
309 consistent with other studies that suggest that unless active upwelling of deeper water is
310 occurring, which can be elevated in DMHg, surface water DMHg values are low due to its loss
311 via gas evasion and also due to some sorts of biotic and abiotic degradation. Overall, given the
312 potential production of MMHg from DMHg photodegradation in either surface waters or in the
313 boundary layer atmosphere, DMHg concentration and flux should be considered a potential
314 mechanism influencing the MMHg pool in local environment, primarily in the atmosphere
315 through its contribution to MMHg dry and wet deposition.^{41, 42}

316 The time series data of dissolved DMHg showed a relative stable trend compared to
317 dissolved Hg⁰ in surface seawater. Dissolved Hg⁰ can be photochemically produced in surface
318 seawater from dissolved divalent Hg, and the observed daily trends of dissolved Hg⁰ support this
319 contention as a diurnal cycle in concentration is evident (Figure 3c).^{44, 45} Conversely, the relative
320 constant dissolved DMHg concentration in surface seawater suggests a stable DMHg source
321 under the surface layer that is not influenced by changes in solar radiation. No strong evidence
322 for photodemethylation of DMHg is found in the data. Further investigation is needed to
323 determine the sources of DMHg in this region. The reason for the elevated concentration of
324 measured dissolved DMHg on Nov 28 is also not known.

325 The air-sea exchange fluxes of both DMHg and Hg⁰ varied similarly and were largely
326 determined by the wind speed as the ambient temperature was relatively consistent over the
327 sampling period, and the change in Hg⁰ concentration was relatively small compared to the
328 differences in wind speed (Supporting Information Figure S3). Due to the supersaturation of
329 DMHg and Hg⁰ in surface seawater, the air-sea exchange flux was always positive, so that the
330 atmosphere was a relative sink for DMHg and Hg⁰. During the wintertime, the coastal region of
331 Long Island Sound can have strong offshore wind during the daytime and higher ambient
332 temperature (surface seawater and atmosphere) due to the solar radiation. Therefore, the trend of
333 air-sea exchange flux could be driven by these changes, i.e. an increasing trend after sunrise with
334 the highest value at midday and the lowest values after sunset.

335

336 **Global comparison and implication.** This study has shown the globally first high-
337 resolution time series data of dissolved DMHg in surface seawater and its air-sea exchange flux.
338 To compare our DMHg measurement with previous studies for the surface ocean (depth < 5 m;
339 Figure 4a), we have extracted previous DMHg data from studies completed in Arctic (red
340 symbol), Pacific (green symbol) and Atlantic (orange symbol) which are representative the polar
341 region, subpolar region, open ocean, upwelling region and coastal region. The dissolved DMHg
342 concentrations of the western Arctic (WA)⁴, Canadian Arctic Archipelago (CAA)¹¹, North Pacific
343 (NP)⁷, central tropical Pacific (CTP)¹⁰, Monterey Bay California (MBC)², North Atlantic (NA)⁵,
344 North Atlantic by Mason (NAM)⁹, South Atlantic (SA)⁸ and Long Island Sound (LIS) averaged
345 15.8 ± 20.9 fM (n = 16), 39.6 ± 59.9 fM (n = 23), 15.6 ± 7.8 fM (n = 5), 9.8 ± 9.7 fM (n = 12),
346 73.3 ± 86.9 fM (n = 15), 43.0 ± 43.3 fM (n = 11), 25.2 ± 45.0 fM (n = 9), 5.3 ± 5.5 fM (n = 6)
347 and 2.6 ± 0.7 fM (n = 438), respectively. In addition, by computing the Tukey Honest Significant
348 Difference of each set of normalized cruise data, four significant different groups of dissolved
349 DMHg were classified as shown in Figure 4b (letter a to d; pairwise confidence level 95%; data
350 shown in Supporting Information Table S2). There was no clear pattern for surface dissolved
351 DMHg in the oceans. However, there were some interesting observations illustrated by the data:
352 1) higher surface dissolved DMHg in CAA than in the WA, 2) equatorial Pacific and equatorial
353 Atlantic generally showed higher dissolved DMHg likely due to the potential Hg supply from the
354 intermediate and deep ocean, 3) the MBC showed the highest dissolved DMHg among all
355 regions, which also suggested the DMHg production at depth and supply to surface, as suggested
356 by others², and 4) coastal region (excluding MBC) apparently had the lowest dissolved DMHg
357 among all regions by a factor of 5 to 10. However, as all previous studies used the traditional
358 manual method, and had higher DL, this may have hindered the accurate determination of
359 DMHg in the surface waters. Indeed, the concentration level of dissolved DMHg in LIS would
360 have been mostly undetectable using the traditional manual method but mostly detectable with
361 our DAA. The successful field measurement with the DAA allowed detection of the low DMHg
362 concentration in surface seawater and such time series of DMHg data should help us better
363 understand the DMHg behavior and its flux from surface seawater to the atmosphere MBL.

364
365

Supporting Information

Detailed descriptions of the algorithm of the peak integration used in the DAA; detailed descriptions of the parameter for air-sea exchange flux calculation of Hg⁰ and DMHg; detailed descriptions of a summary of previous published data used in the global comparison in this study; an example of the peak signal from the data logger (black line) and the fitted curve using a log normal distribution (red line) with the marked start and end points (vertical blue line) for Hg⁰ and DMHg peak, respectively; a case of the Carbotrap deployment for measuring breakthrough; detailed descriptions of ancillary surface seawater and atmospheric data for the field measurement at coastal Long Island Sound including surface seawater temperature and wind speed, from top panel to bottom panel, respectively.

Acknowledgments

We would like to thank Zofia Baumann, Bridget Holohan, Dennis Arbige, Robert Dziomba, Charles Woods, Kay Howard-Strobel, Prentiss Balcom and others who helped with this study.

This study was partially funded by the National Science Foundation (NSF) Chemical Oceanography Program (Grant # 1736659) and Polar Programs (Grant # 1854454) and the University of Connecticut Predoctoral Fund.

References

1. Mason, R.; Fitzgerald, W., Alkylmercury species in the equatorial Pacific. *Nature* **1990**, *347*, (6292), 457-459.
2. Conaway, C. H.; Black, F. J.; Gault-Ringold, M.; Pennington, J. T.; Chavez, F. P.; Flegal, A. R., Dimethylmercury in Coastal Upwelling Waters, Monterey Bay, California. *Environmental Science & Technology* **2009**, *43*, (5), 1305-1309.
3. Kirk, J. L.; Lehnerr, I.; Andersson, M.; Braune, B. M.; Chan, L.; Dastoor, A. P.; Durnford, D.; Gleason, A. L.; Loseto, L. L.; Steffen, A., Mercury in Arctic marine ecosystems: Sources, pathways and exposure. *Environmental research* **2012**, *119*, 64-87.
4. Agather, A. M.; Bowman, K. L.; Lamborg, C. H.; Hammerschmidt, C. R., Distribution of mercury species in the Western Arctic Ocean (U.S. GEOTRACES GN01). *Marine Chemistry* **2019**, *216*, 103686.
5. Bowman, K. L.; Hammerschmidt, C. R.; Lamborg, C. H.; Swarr, G., Mercury in the North Atlantic Ocean: The U.S. GEOTRACES zonal and meridional sections. *Deep Sea Research Part II: Topical Studies in Oceanography* **2015**, *116*, 251-261.
6. Bowman, K. L.; Hammerschmidt, C. R.; Lamborg, C. H.; Swarr, G. J.; Agather, A. M., Distribution of mercury species across a zonal section of the eastern tropical South Pacific Ocean (U.S. GEOTRACES GP16). *Marine Chemistry* **2016**, *186*, 156-166.
7. Hammerschmidt, C. R.; Bowman, K. L., Vertical methylmercury distribution in the subtropical North Pacific Ocean. *Marine Chemistry* **2012**, *132-133*, 77-82.
8. Mason, R. a.; Sullivan, K., The distribution and speciation of mercury in the South and equatorial Atlantic. *Deep Sea Research Part II: Topical Studies in Oceanography* **1999**, *46*, (5), 937-956.
9. Mason, R. P.; Rolfhus, K. R.; Fitzgerald, W. F., Mercury in the North Atlantic. *Marine Chemistry* **1998**, *61*, (1), 37-53.
10. Munson, K. M.; Lamborg, C. H.; Swarr, G. J.; Saito, M. A., Mercury species concentrations and fluxes in the Central Tropical Pacific Ocean. *Global Biogeochemical Cycles* **2015**, *29*, (5), 656-676.
11. Kirk, J. L.; St. Louis, V. L.; Hintelmann, H.; Lehnerr, I.; Else, B.; Poissant, L., Methylated Mercury Species in Marine Waters of the Canadian High and Sub Arctic. *Environmental Science & Technology* **2008**, *42*, (22), 8367-8373.
12. Pongratz, R.; Heumann, K. G., Production of methylated mercury, lead, and cadmium by marine bacteria as a significant natural source for atmospheric heavy metals in polar regions. *Chemosphere* **1999**, *39*, (1), 89-102.
13. Pak, K.-R.; Bartha, R., Mercury Methylation and Demethylation in Anoxic Lake Sediments and by Strictly Anaerobic Bacteria. *Applied and Environmental Microbiology* **1998**, *64*, (3), 1013-1017.
14. Eckley, C. S.; Hintelmann, H., Determination of mercury methylation potentials in the water column of lakes across Canada. *Science of The Total Environment* **2006**, *368*, (1), 111-125.
15. Mason, R. P.; Fitzgerald, W. F., The distribution and biogeochemical cycling of mercury in the equatorial Pacific Ocean. *Deep Sea Research Part I: Oceanographic Research Papers* **1993**, *40*, (9), 1897-1924.
16. Mason, R. P.; Fitzgerald, W. F., Mercury speciation in open ocean waters. *Water Air & Soil Pollution* **1991**, *56*, (1), 779-789.

17. Campbell, L. M.; Norstrom, R. J.; Hobson, K. A.; Muir, D. C.; Backus, S.; Fisk, A. T., Mercury and other trace elements in a pelagic Arctic marine food web (Northwater Polynya, Baffin Bay). *Science of the Total Environment* **2005**, *351*, 247-263.
18. Mason, R. P.; Reinfelder, J. R.; Morel, F. M. M., Bioaccumulation of mercury and methylmercury. *Water, Air, and Soil Pollution* **1995**, *80*, (1), 915-921.
19. Hammerschmidt, C. R.; Lamborg, C. H.; Fitzgerald, W. F., Aqueous phase methylation as a potential source of methylmercury in wet deposition. *Atmospheric Environment* **2007**, *41*, (8), 1663-1668.
20. Weiss-Penzias, P.; Coale, K.; Heim, W.; Fernandez, D.; Oliphant, A.; Dodge, C.; Hoskins, D.; Farlin, J.; Moranville, R.; Olson, A., Total- and monomethyl-mercury and major ions in coastal California fog water: Results from two years of sampling on land and at sea. *Elementa: Science of the Anthropocene* **2016**, *4*, 000101.
21. Baya, P. A.; Gosselin, M.; Lehnerr, I.; St Louis, V. L.; Hintelmann, H., Determination of monomethylmercury and dimethylmercury in the Arctic marine boundary layer. *Environ Sci Technol* **2015**, *49*, (1), 223-32.
22. Mason, R. P.; Fitzgerald, W. F.; Vandal, G. M., The sources and composition of mercury in Pacific Ocean rain. *Journal of Atmospheric Chemistry* **1992**, *14*, (1), 489-500.
23. Coale, K. H.; Heim, W. A.; Negrey, J.; Weiss-Penzias, P.; Fernandez, D.; Olson, A.; Chiswell, H.; Byington, A.; Bonnema, A.; Martenuk, S.; Newman, A.; Beebe, C.; Till, C., The distribution and speciation of mercury in the California current: Implications for mercury transport via fog to land. *Deep Sea Research Part II: Topical Studies in Oceanography* **2018**, *151*, 77-88.
24. Pongratz, R.; Heumann, K. G., Determination of Concentration Profiles of Methyl Mercury Compounds in Surface Waters of Polar and other Remote Oceans by GC-AFD. *International Journal of Environmental Analytical Chemistry* **1998**, *71*, (1), 41-56.
25. Parker, J. L.; Bloom, N. S., Preservation and storage techniques for low-level aqueous mercury speciation. *Science of The Total Environment* **2005**, *337*, (1), 253-263.
26. Bloom, N.; Fitzgerald, W. F., Determination of volatile mercury species at the picogram level by low-temperature gas chromatography with cold-vapour atomic fluorescence detection. *Analytica Chimica Acta* **1988**, *208*, 151-161.
27. M. Tseng, C.; de Diego, A.; Pinaly, H.; Amouroux, D.; F. X. Donard, O., Cryofocusing coupled to atomic absorption spectrometry for rapid and simple mercury speciation in environmental matrices. *Journal of Analytical Atomic Spectrometry* **1998**, *13*, (8), 755-764.
28. Fischer, R.; Rapsomanikis, S.; Andreae, M. O., Determination of methylmercury in fish samples using GC/AA and sodium tetraethylborate derivatization. *Analytical Chemistry* **1993**, *65*, (6), 763-766.
29. Hintelmann, H.; Evans, R. D.; Villeneuve, J. Y., Measurement of mercury methylation in sediments by using enriched stable mercury isotopes combined with methylmercury determination by gas chromatography–inductively coupled plasma mass spectrometry. *Journal of Analytical Atomic Spectrometry* **1995**, *10*, (9), 619-624.
30. Szpunar, J.; Łobiński, R.; Wasik, A.; Rodriguez Pereiro, I.; Dietz, C., Speciation of mercury by ICP-MS after on-line capillary cryofocussing and ambient temperature multicapillary gas chromatography. *Analytical Communications* **1998**, *35*, (10), 331-335.
31. Black, F. J.; Conaway, C. H.; Flegal, A. R., Stability of Dimethyl Mercury in Seawater and Its Conversion to Monomethyl Mercury. *Environmental Science & Technology* **2009**, *43*, (11), 4056-4062.

32. Nierenberg, D. W.; Nordgren, R. E.; Chang, M. B.; Siegler, R. W.; Blayney, M. B.; Hochberg, F.; Toribara, T. Y.; Cernichiari, E.; Clarkson, T., Delayed Cerebellar Disease and Death after Accidental Exposure to Dimethylmercury. *New England Journal of Medicine* **1998**, *338*, (23), 1672-1676.
33. Siegler, R. W.; Nierenberg, D. W.; Hickey, W. F., Fatal poisoning from liquid dimethylmercury: A neuropathologic study. *Human Pathology* **1999**, *30*, (6), 720-723.
34. Andersson, M. E.; Gårdfeldt, K.; Wängberg, I., A description of an automatic continuous equilibrium system for the measurement of dissolved gaseous mercury. *Analytical and Bioanalytical Chemistry* **2008**, *391*, (6), 2277.
35. DiMento, B. P.; Mason, R. P.; Brooks, S.; Moore, C., The impact of sea ice on the air-sea exchange of mercury in the Arctic Ocean. *Deep Sea Research Part I: Oceanographic Research Papers* **2019**, *144*, 28-38.
36. Mason, R. P.; Hammerschmidt, C. R.; Lamborg, C. H.; Bowman, K. L.; Swarr, G. J.; Shelley, R. U., The air-sea exchange of mercury in the low latitude Pacific and Atlantic Oceans. *Deep Sea Research Part I: Oceanographic Research Papers* **2017**, *122*, 17-28.
37. Soerensen, A. L.; Mason, R. P.; Balcom, P. H.; Jacob, D. J.; Zhang, Y.; Kuss, J.; Sunderland, E. M., Elemental Mercury Concentrations and Fluxes in the Tropical Atmosphere and Ocean. *Environmental Science & Technology* **2014**, *48*, (19), 11312-11319.
38. Baya, P. A.; Hollinsworth, J. L.; Hintelmann, H., Evaluation and optimization of solid adsorbents for the sampling of gaseous methylated mercury species. *Anal Chim Acta* **2013**, *786*, 61-9.
39. Schartup, A. T.; Balcom, P. H.; Soerensen, A. L.; Gosnell, K. J.; Calder, R. S. D.; Mason, R. P.; Sunderland, E. M., Freshwater discharges drive high levels of methylmercury in Arctic marine biota. *Proceedings of the National Academy of Sciences* **2015**, *112*, (38), 11789-11794.
40. Schartup, A. T.; Balcom, P. H.; Mason, R. P., Sediment-Porewater Partitioning, Total Sulfur, and Methylmercury Production in Estuaries. *Environmental Science & Technology* **2014**, *48*, (2), 954-960.
41. Balcom, P. H.; Fitzgerald, W. F.; Vandal, G. M.; Lamborg, C. H.; Rolffhus, K. R.; Langer, C. S.; Hammerschmidt, C. R., Mercury sources and cycling in the Connecticut River and Long Island Sound. *Marine Chemistry* **2004**, *90*, (1), 53-74.
42. Balcom, P. H.; Schartup, A. T.; Mason, R. P.; Chen, C. Y., Sources of water column methylmercury across multiple estuaries in the Northeast U.S. *Marine Chemistry* **2015**, *177*, 721-730.
43. Gosnell, K. J.; Balcom, P. H.; Tobias, C. R.; Gilhooly III, W. P.; Mason, R. P., Spatial and temporal trophic transfer dynamics of mercury and methylmercury into zooplankton and phytoplankton of Long Island Sound. *Limnology and Oceanography* **2017**, *62*, (3), 1122-1138.
44. Mason, R. P., Air-sea Exchange and Marine Boundary Layer Atmospheric Transformation of Hg and their Importance in the Global Mercury Cycle. In *Dynamics of Mercury Pollution on Regional and Global Scales: Atmospheric Processes and Human Exposures Around the World*, Pirrone, N.; Mahaffey, K. R., Eds. Springer US: Boston, MA, 2005; pp 213-239.
45. Fitzgerald, W. F.; Gill, G. A.; Kim, J. P., An Equatorial Pacific Ocean Source of Atmospheric Mercury. *Science* **1984**, *224*, (4649), 597.

Table 1. *The dimethylmercury automatic analyzer settings and the analytical parameters used and validated in this study.*

Sampling cycle	
Seawater inflow	10 – 15 L/min
Pressurized air	1.1 – 1.2 L/min (Hg free)
Temperature sensor	HOBO MX2201 (1 Hz, ± 0.5 °C)
Drying tube	Soda lime (5.0 g, 4 – 8 mesh)
Sample trap	Carbotrap B (0.1 g, 20 – 40 mesh)
Sampling duration	30 min

Desorption cycle	
Carrier gas	Argon (UHP)
Carrier flow rate	60 ± 2 ml/min
Desorption temperature	250 ± 10 °C (30 sec)
GC column	Teflon tube (1 m length, $\frac{1}{4}$ inch OD)
GC column temperature	38 ± 1 °C
Pyrolyzer column	Quartz tube (15 cm length, $\frac{1}{4}$ inch OD)
Pyrolyzer temperature	700 ± 50 °C
Retention time of Hg ⁰	75 sec
Retention time of DMHg	160 sec
Desorption duration	5 min

Detector and data logger	
Detector	CVAFS (Tekran 2500)
Data logger	PeakSimple (Model 333)
Peak integration	LabVIEW or other software

List of Figures

Figure 1. Schematic diagram of the apparatus for measuring dissolved dimethylmercury (DMHg) in seawater: (a) The newly developed DMHg automatic analyzer (DAA) couples the main sampling and analytic steps, including a continuous flow chamber, dual Carbotrap pre-concentration, a gas chromatographic column, a cold vapor atomic fluorescence spectrometer and a data logger. V1, V2, V3 and V4 represent the solenoid valve and switch the flow based on the analytical cycle. The whole system allows the simultaneous measurement of dissolved DMHg and dissolved Hg^0 at different time resolution; (b) The traditional manual analytic method couples the main sampling and manual analytic steps, which are the same as outlined in a) above but requires a specified time for the change of the Carbotrap for each batch sampling.

Figure 2. (a) Plot of the breakthrough recovery on the Carbotrap with the increasing sampling volume of air including data from a previous study (Baya, Hollinsworth and Hintelmann³⁸; orange cycle) and this study (blue cycle). The fitted polynomial line and the 95% confidence level area (red line; grey area) are denoted ($R^2 = 0.96$, $p < 0.001^{***}$). (b) The relative variation of the 3-day interval calibration of the system from day 0 to day 15 (blue bar). The horizontal grey area shows the $\pm 5\%$ relative variation from the average value.

Figure 3. The sampling site of the field measurement and results for the dimethylmercury automatic analyzer (DAA) for one week at Avery Point, CT, from Nov 23 to Nov 29, 2021. (a) The USA map with the relative location of Long Island Sound marked with the black rectangle and the Long Island Sound map with the sampling point indicated (red dot) and with the colored bathymetric depth and terrestrial altitude indicated, which were obtained from the National Centers for Environmental Information (NCEI) of the National Oceanic and Atmospheric Administration (NOAA). (b) Dissolved DMHg measured by DAA (30-minute integrations, grey dot) and 5-hour moving average (light blue line). (c) Dissolved Hg^0 concentration measured by DAA (5-minute integrations, grey dot) and 5-hour moving average (light red line). (d) The air-sea exchange flux of DMHg in surface seawater calculated based on the DAA

measurement (blue line). (e) The air-sea exchange flux of Hg^0 in surface seawater calculated based on the DAA measurement (red line). The environmental parameters associated with this field measurement are summarized and shown in Supporting Information Figure S3.

Figure 4. Global dimethylmercury (DMHg) measurements in the surface ocean mixed layer (<5 m) from the past 30-years of published studies. (a) Summarized DMHg measurement completed in the Arctic (red symbol), Pacific (green symbol) and Atlantic Oceans (orange symbol). The abbreviations are: western Arctic (WA), Canadian Arctic Archipelago (CAA), North Pacific (NP), central tropical Pacific (CTP), Monterey Bay, California (MBC), North Atlantic (NA), North Atlantic, data by Mason (NAM), South Atlantic (SA) and Long Island Sound (LIS). (b) Comparisons of dissolved DMHg concentration in surface seawater in the global ocean. Different letters (a to d) denote significant differences between locations for the normalized data; that is, for two groups with different letters, their mean values are significantly different at the $p < 0.05^*$ level (Tukey Honest Significant Difference). Previous published data and the references for each study are provided in Supporting Information Table S2.

Graphical Abstract

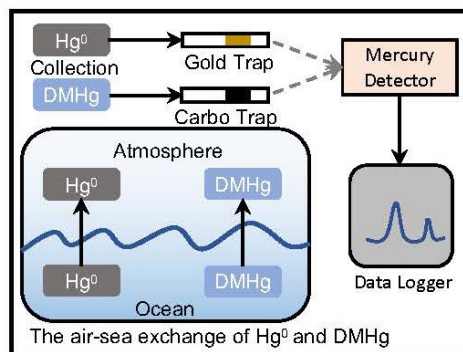


Figure 1

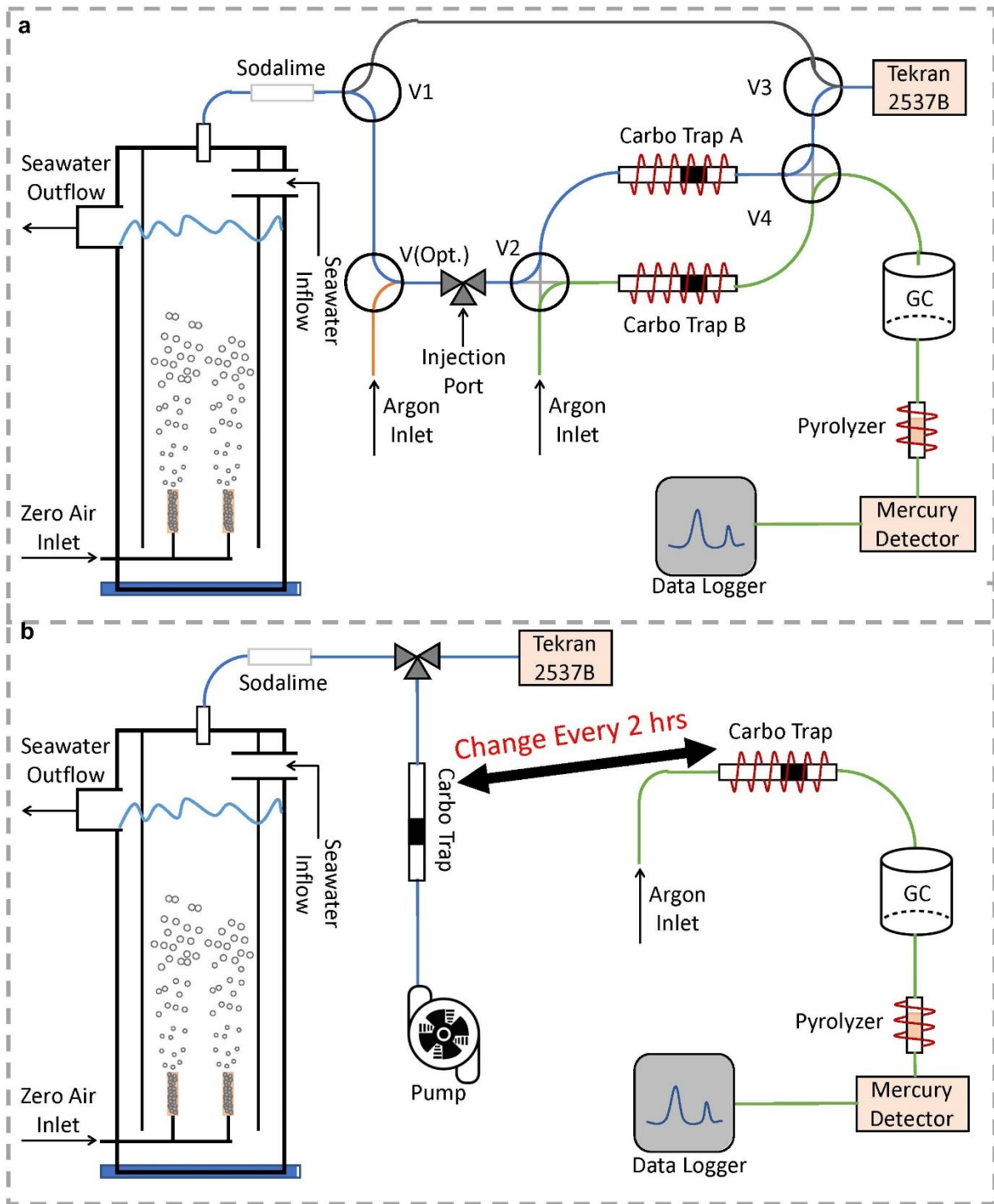
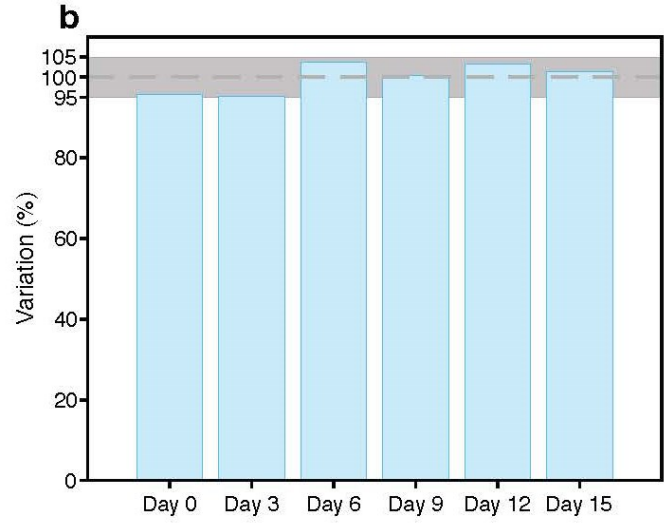
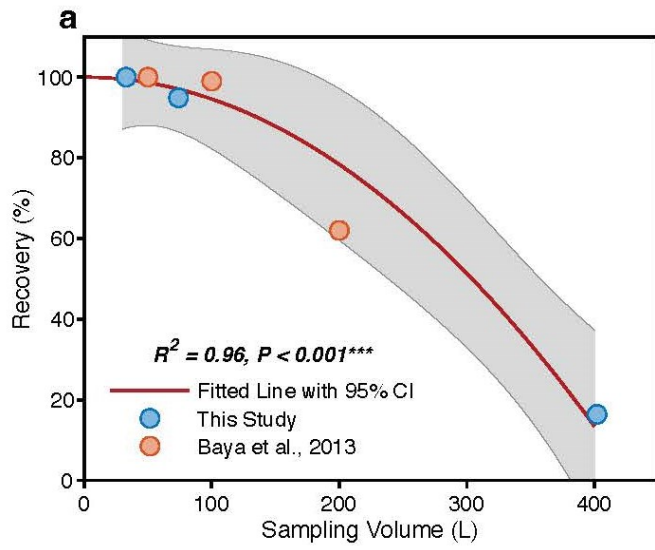


Figure 2



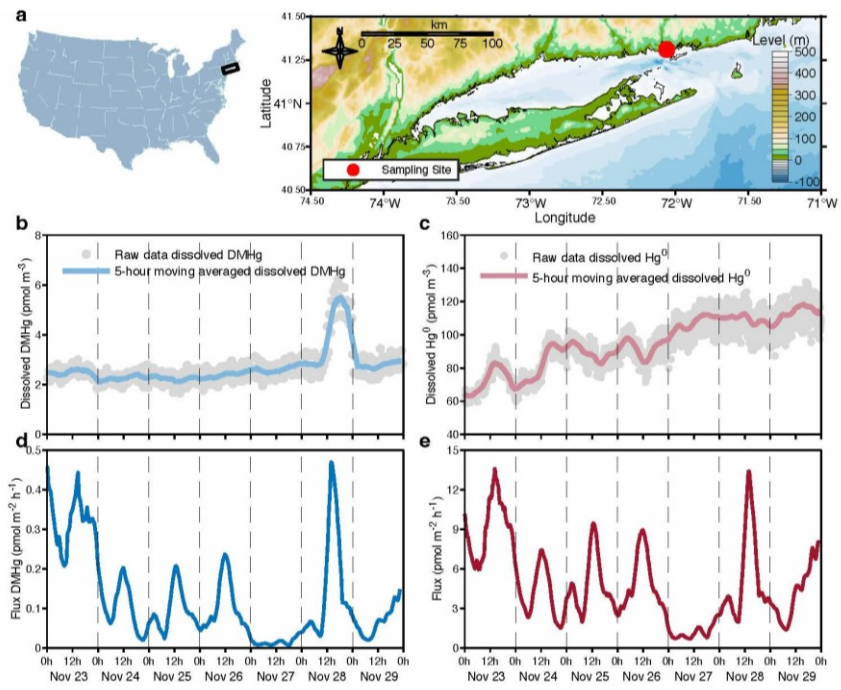


Figure 3 (Double-column)

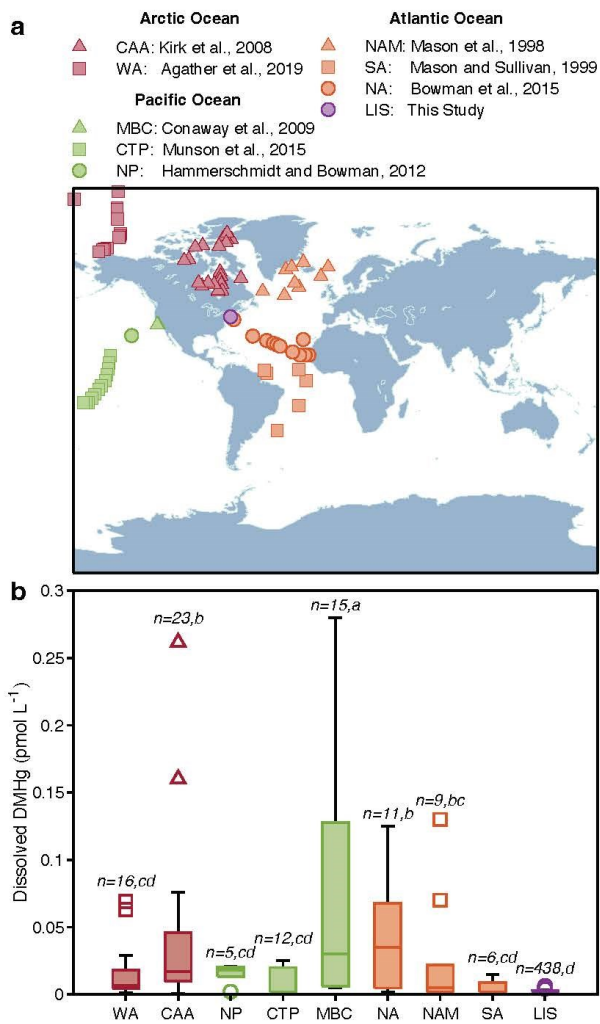


Figure 4 (Single-column)